Measuring the quantum state of a photon pair entangled in frequency and time

Alex O. C. Davis, Valerian Thiel, Brian J. Smith

Research Article Vol. 7, No. 10 / October 2020 / Optica 1317

optica

Measuring the quantum state of a photon pair entangled in frequency and time

ALEX O. C. DAVIS,[1,2,*,†] VALÉRIAN THIEL,[1,3,†] AND BRIAN J. SMITH[1,3]

[1]Clarendon Laboratory, University of Oxford, Parks Road, Oxford OX1 3PU, UK
[2]Laboratoire Kastler Brossel, UPMC-Sorbonne Universités, CNRS, ENS-PSL Research University, Collége de France, 75005 Paris, France
[3]Department of Physics and Oregon Center for Optical, Molecular, and Quantum Science, University of Oregon, Eugene, Oregon 97403, USA
*Corresponding author: alex.davis@lkb.upmc.fr

Received 4 May 2020; revised 3 August 2020; accepted 7 September 2020 (Doc. ID 396933); published 30 September 2020

Quantum entanglement plays a prominent role in both foundational physics and emerging quantum technologies. Light is especially promising as a platform for experimental realizations of high-dimensional entanglement, for which the time-frequency degree of freedom provides a natural encoding. Here, we propose and demonstrate a technique to determine the full quantum state of a pair of photons entangled in the time-frequency domain. Our approach, based on spectral shearing interferometry, is entirely self-referenced. To test our system, we measure a photon-pair source with nonlocal spectral phase that results in entanglement between the photons, in which the time when either photon is detected is correlated with the frequency of the other photon. The results demonstrate an effective new tool for exploring the temporal and spectral characteristics of multipartite quantum systems exhibiting high-dimensional entanglement.

https://doi.org/10.1364/OPTICA.396933

1. INTRODUCTION

Entanglement is not only a fundamental signature of quantum physics, but an essential resource in emerging quantum technologies [1]. High-dimensional entangled states of light are of interest as a resource for a range of tasks, such as quantum computation [2], quantum key distribution (QKD) [3], quantum communications [4], and dense coding [5]. The ability to fully characterize such states is of widespread interest both for the development and implementation of such technologies and to enable tests of the foundations of quantum theory [6].

Quantum correlations between photon pairs can arise in any of the physical degrees of freedom of light, including polarization [7], spatial mode [8], and the longitudinal or time-frequency (TF) mode. The TF degree of freedom has recently gained significant interest as a basis for encoding quantum information due to its large accessible dimensionality and compatibility with integrated optical platforms [9]. High-dimensional TF entangled photon pairs, which can display tight correlations in time and frequency, have emerged as a useful resource for QKD [3,10], quantum-enhanced sensing [11], nonlinear spectroscopy [12], and quantum range-finding protocols [13]. In addition, high-dimensional entangled systems offer advantages over entangled qubit systems in foundational tests based on violation of generalized Bell inequalities [14].

These protocols require well-characterized sources and detectors of entangled light, the development and evaluation of which demands a measurement scheme that is sensitive to nonclassical correlations [15,16]. Additionally, the intermediate devices that form the building blocks of quantum networks, such as quantum repeaters and memories, must be verified to conserve the fragile nonlocal coherences of their input states [17]. A complete characterization scheme for TF entangled photons is therefore of considerable interest for the development of quantum technologies that employ optical TF encoding.

Measurements that achieve partial characterization of joint spectral-temporal properties of two-photon states have been recently demonstrated [18,19]. Joint spectral intensity (JSI) measurement, which gives the probability of detecting the photons with given frequencies, is now a standard characterization method [15]. The joint temporal intensity (JTI), which gives the probability of detecting the photons at given arrival times, is more challenging to measure for broadband light, as the timescales involved can be on the order of tens to hundreds of femtoseconds. Both of these measurements are insensitive to phase and hence cannot reveal the full extent of possible nonclassical correlations [15]. Taken together, joint measurements in both frequency and time have enabled partial characterization of entangled ultrafast photon pairs [19], but still cannot provide the full two-photon state. Recently, complete characterization of restricted classes of two-photon states with frequency correlations has been achieved by either time-resolved [20] or frequency-resolved [21] two-photon interference measurements. This approach is limited to nearly degenerate, tightly correlated photon-pair sources with joint temporal amplitudes that depend only on the two-photon time difference and cannot address each photon independently. A recent demonstration employing sum frequency generation with classical

reference fields achieved full characterization, at the experimental price of prohibitive group velocity and phase matching conditions and stable and well-characterized reference fields [22].

Here, we demonstrate a self-referencing method to fully characterize the state of an entangled two-photon system based upon our recent approach to single-photon state characterization by electro-optic shearing interferometry [23,24]. In a previous experiment, we used this method to reconstruct the complex spectral amplitude $\psi(\omega)$ of a classical field mode occupied by a heralded single photon. Here, we incorporate this photon-level classical field mode reconstruction into a coincident detection scheme to fully characterize the TF state of a spectrally entangled photon pair. This is achieved by performing spectrally resolved measurements of one photon in coincidence with an interferometric measurement of the other that is sensitive to the spectral phase. This method remains fully self-referenced, introduces no constraints on the mode overlap between the two photons themselves, and relies on single-photon interference enabling nonlocal correlations to be directly observed. This approach to determine the quantum state of photon pairs will enable further development of novel ways for generating, manipulating, and measuring high-dimensional quantum systems. We anticipate that this work will unlock new opportunities for both quantum technology and fundamental studies of quantum mechanics with entangled quantum systems.

A general two-photon pure state $|\Psi\rangle$ can be expressed in terms of the complex-valued joint spectral amplitude (JSA) $f(\omega_1, \omega_2)$, which is also called the two-photon spectral-temporal wave function,

$$|\Psi\rangle = \iint f(\omega_1, \omega_2)\hat{a}_s^\dagger(\omega_2)\hat{a}_i^\dagger(\omega_1)\mathrm{d}\omega_1\mathrm{d}\omega_2|\mathrm{vac}\rangle, \qquad (1)$$

where $\hat{a}_s^\dagger(\omega_2)$ and $\hat{a}_i^\dagger(\omega_1)$ are bosonic operators that create photons in two orthogonal modes (termed "signal" and "idler") with frequencies ω_2 and ω_1, respectively, and $|\mathrm{vac}\rangle$ is the vacuum state of the electromagnetic field. The JSI is given by the square modulus of the JSA, $S(\omega_1, \omega_2) \equiv |f(\omega_1, \omega_2)|^2$. Additionally, the JSA is characterized by the joint spectral phase, $\phi(\omega_1, \omega_2) \equiv \mathrm{Arg}[f(\omega_1, \omega_2)]$. The joint spectral phase $\phi(\omega_1, \omega_2)$ may be expanded as a power series about the central frequencies of the two photons ω_{c1} and ω_{c2},

$$\phi(\omega_1, \omega_2) = \phi_{00} + \phi_{10}\tilde{\omega}_1 + \phi_{01}\tilde{\omega}_2 + \phi_{11}\tilde{\omega}_1\tilde{\omega}_2 + \phi_{20}\tilde{\omega}_1^2 + \phi_{02}\tilde{\omega}_2^2 + \ldots,$$

where $\omega_1 = \omega_{c1} + \tilde{\omega}_1$, $\omega_2 = \omega_{c2} + \tilde{\omega}_2$, and $\phi_{00} \equiv \phi(\omega_{c1}, \omega_{c2})$ is the uncharacterized global phase. This is a complete description of the joint spectral phase in terms of the signal and idler central frequencies and expansion coefficients $\{\phi_{ij}\}$. The terms in this expansion with coefficients ϕ_{0j} or ϕ_{i0} are independent of the frequency of one photon and give the classical spectral phase of separable photons. The remaining coefficients ϕ_{ij}, for which $\{i, j\} \neq 0$, are collectively referred to here as the *nonlocal spectral phase*. These coefficients encode TF entanglement and are invariant under local phase operations on either photon.

Our approach to measuring $f(\omega_1, \omega_2)$ is based on the electro-optic spectral shearing interferometer (EOSI). Widely used in classical ultrafast pulse characterization, spectral shearing interferometry is appealing, as the lack of an external optical reference field allows for more rapid characterization with a simpler experimental set-up [25,26]. Our previous demonstration of EOSI used electro-optic spectral shearing to extend these benefits to the characterization of single-photon-level pulses [24]. The experimental concept for the full two-photon state characterization incorporates EOSI and is illustrated in Fig. 1. Initially, the idler photon passes through an EOSI comprised of a Mach–Zehnder interferometer, where one path undergoes a spectral shear, Ω, and the other path imparts a relative delay, τ. The spectral shear is applied using an electro-optic modulator (EOM), the deterministic nature of which ensures unit internal efficiency of the frequency translation. The output of the interferometer is monitored by a single-photon-counting spectrometer registering frequency ω_1. The signal photon is simultaneously monitored by a second single-photon-counting spectrometer registering frequency ω_2. The JSI of the idler photon upon emerging from one port of the EOSI and the signal photon is then

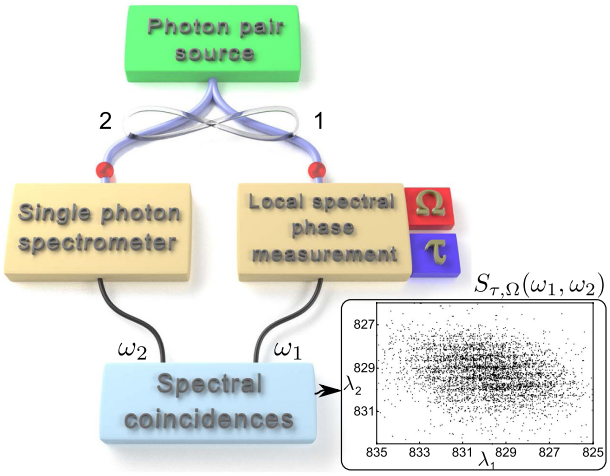

Fig. 1. Experimental concept. Spatially separated beams containing the signal and idler photons are measured using frequency-resolved measurements at the output of an electro-optic shearing interferometer registering ω_1 providing local spectral phase information and a single-photon-counting spectrometer registering ω_2. The measured joint spectral interference distribution (inset) follows the expression in Eq. (2).

$$S_{\tau,\Omega}(\omega_1, \omega_2) = \frac{1}{4}\{S(\omega_1, \omega_2) + S(\omega_1 + \Omega, \omega_2) + 2\mathrm{Re}[f(\omega_1, \omega_2)f^*(\omega_1 + \Omega, \omega_2)e^{i\omega_1\tau}]\}. \qquad (2)$$

The joint spectral phase difference,

$$\phi(\omega_1 + \Omega, \omega_2) - \phi(\omega_1, \omega_2) = \mathrm{Arg}[f(\omega_1, \omega_2)f^*(\omega_1 + \Omega, \omega_2)],$$

can be extracted from the spectral interference term in Eq. (2) using Fourier transform filtering techniques in [26] and Supplement 1. From this phase difference measurement, it is possible to reconstruct $\phi(\omega_1, \omega_2)$ up to an additive term that is a function of ω_2 only (specifically, the terms with coefficients ϕ_{0j}). This term can be determined by repeating the measurement with the paths of the signal and idler photons exchanged. The JSI and the relative phase of the complex JSA $f(\omega_1, \omega_2)$ can thus be determined from these measurements.

2. EXPERIMENTAL METHODS

To demonstrate our method for measuring the complex JSA, we prepare photon pairs with nearly factorable (uncorrelated)

JSI $S(\omega_1, \omega_2) \approx |\psi(\omega_1)|^2 |\chi(\omega_2)|^2$ using spontaneous parametric down conversion (SPDC) [27], but with tunable joint spectral phase. The photon-pair source is designed such that the JSA $f(\omega_1, \omega_2)$ is separable when the SPDC process is pumped by a transform-limited pulse. Spectral phase correlations in the complex JSA $f(\omega_1, \omega_2)$ can be introduced by controlling the pump spectral phase. Here, the entanglement of the photon-pair source is controlled by adjusting the pump quadratic spectral phase (see Supplement 1), and the JSA may be written as $f(\omega_1, \omega_2) = \bar{\psi}(\omega_1)\bar{\chi}(\omega_2)\exp\{i\phi_p\omega_1\omega_2\}$, where $\bar{\psi}(\omega_1)$ ($\bar{\chi}(\omega_2)$) contain local quadratic spectral phase for the idler (signal) photon. The nonlocal phase term introduced, $i\phi_p\omega_1\omega_2$, may be interpreted as a time delay on either photon that varies with the frequency of the other photon, and so it creates correlations whereby the outcomes of spectral measurements on either photon are correlated with the arrival time of the other and vice versa. This correlation term is unaffected by local unitary operations on either daughter photon after preparation.

A detailed schematic of the experimental setup is shown in Fig. 2. The photon-pair source is based upon collinear, Type-II phase-matched SPDC in a potassium dihydrogen phosphate (KDP) crystal [27]. The idler and signal photons are generated in orthogonal polarizations at an 830 nm central wavelength with marginal full width at half-maximum (FWHM) bandwidth of 2.5 nm and 7.5 nm, respectively. The joint TF state of the photon pair can be assumed to be pure and hence can be represented in the form of Eq. (1). The purity of the photon-pair state will be affected primarily by fluctuations of the pump pulses. The crystal is pumped by femtosecond pulses of 415 nm central wavelength derived from a frequency-doubled titanium sapphire (Ti:Sapph) laser. A prism stretcher-compressor in the pump path capable of applying a negative group delay dispersion up to $\phi_p = -1.5 \times 10^5$ fs^2 enables the introduction of variable quadratic spectral phase to the pump.

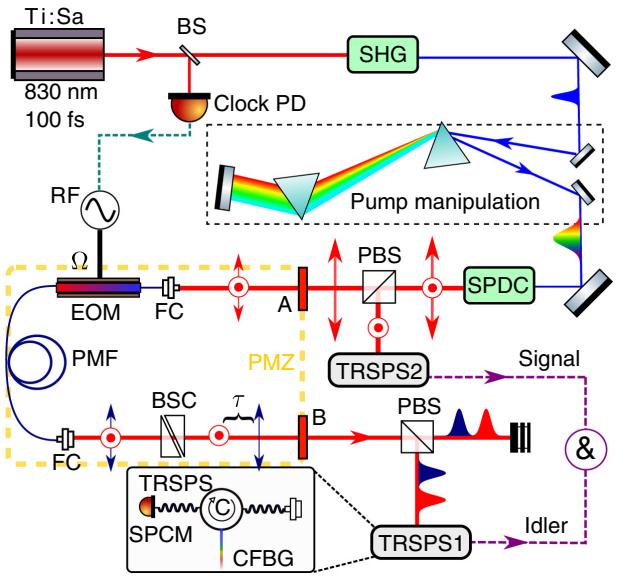

Fig. 2. Experimental setup Ti:Sa, Ti:Sapphire laser; (P)BS, (polarizing) beam splitter; PD, fast photodiode; RF, radio-frequency driving electronics; EOM, electro-optic phase modulator; Ω frequency shear; SHG, second harmonic generation; SPDC, spontaneous parametric down conversion; A and B, half-wave plates, respectively, opening and closing the polarization Mach–Zehnder interferometer (PMZ); PMF, polarization maintaining fiber; BSC, Babinet–Soleil compensator; FC, fiber coupling; τ, time delay; TRSPS, time-resolved single-photon spectrometer; &, coincidence electronics. **Inset: Time-resolved single-photon-counting spectrometer** C, optical circulator; CFBG, chirped fiber Bragg grating; SPCM, single-photon-counting module.

To characterize the JSA of the SPDC source, the co-propagating signal and idler photons are separated at a polarizing beam splitter (PBS). The signal photon is directed into a time-resolved single-photon spectrometer (TRSPS) [28], which performs a frequency-resolved measurement. The idler photon is sent into the EOSI. The collinear paths of the interferometer are distinguished by polarization (Supplement 1 and [23,24]). Frequency-resolved measurement at one output of the EOSI is performed by another TRSPS and logged in coincidence with the measurement outcomes for the signal photon. This joint measurement is repeated for many copies of the two-photon state until significant coincidence count statistics are obtained, such that interference fringes can be observed. These data, which are an estimate of the JSI in Eq. (2), may then be represented as a two-dimensional histogram showing spectral interference fringes (see Fig. 1). This dataset suffices to reconstruct the joint spectral phase $\phi(\omega_1, \omega_2)$ up to a function of ω_2 only, which can be determined by reversing the role of signal and idler in the experiment. We describe the inversion procedure in Supplement 1.

3. RESULTS

In the case of the chirped pump when the idler photon is launched into the EOSI, the position of these fringes varies as a function of ω_2, giving them a diagonal slant, as seen in Fig. 3. This dependency is due to the nonlocal spectral phase $\phi_{11}\omega_1\omega_2$, with $\phi_{11} = \phi_p$.

We can determine the expansion coefficients using the methods laid out in Supplement 1. The parameters ϕ_{01} and ϕ_{10} give the local linear spectral phase on each photon, which represents the arrival time of the photon into the interferometer with respect to the zero crossing of the radio-frequency waveform in the EOM. In our implementation, these parameters were chosen to be zero to maximize the spectral shear on the wave packet.

From the measurement in which the idler is sent to the EOSI, the correlated nonlocal phase parameter is found to be $\phi_{11} = (-1.61 \pm 0.08) \cdot 10^5$ fs^2, and the local quadratic spectral phase is $2\phi_{20} = (-1.42 \pm 0.2) \cdot 10^5$ fs^2, which should both equal the spectral phase introduced by the prism stretcher $\phi_p = -1.5 \cdot 10^5$ fs^2, showing good agreement with the value of ϕ_p determined from the design of the prism stretcher.

Changing the role of the signal and idler photon in the experiment, the signal photon was injected into the EOSI and measured in coincidence with the spectrally resolved idler photon. Fringes are then observed along the shorter bandwidth of the joint spectrum (see Fig. 3). Our analysis retrieves values of $\phi_{11} = (-1.45 \pm 0.2) \cdot 10^5$ fs^2 and $2\phi_{02} = (-1.25 \pm 0.1) \cdot 10^5$ fs^2, consistent with the theoretical predictions that these should equal the chirp on the pump (Supplement 1). The nonlocal phase parameter ϕ_{11} is recovered in both configurations and should be consistent between them and is equal to the chirp of the pump ϕ_p. The measured values of these parameters are within experimental uncertainties. The larger uncertainty on ϕ_{11} occurs when the narrow-bandwidth photon is sent to the EOSI, since the interferogram then has fewer spectral fringes leading to a less stable reconstruction. No significant higher-order spectral phase was observed.

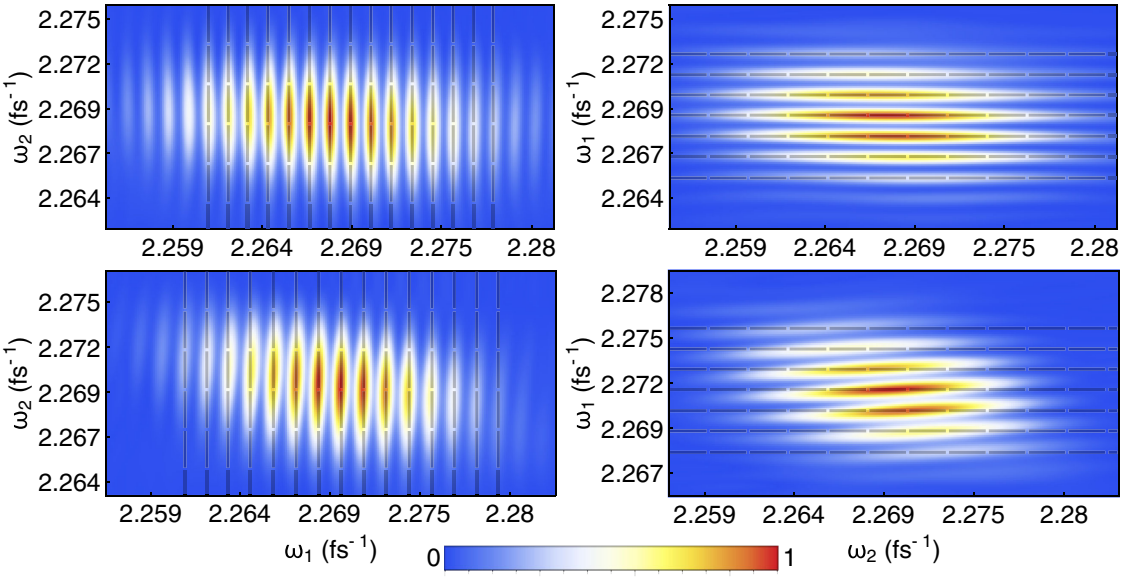

Fig. 3. Experimental low pass filtered joint spectral interferograms for both daughter photons of the SPDC in the case of an unchirped (top) and chirped (bottom) pump, representing a typical 6 min acquisition. A color map shows JSI normalized to the maximum. Diagonal fringes in the chirped pump case are indicative of spectral phase correlations between the two photons. Dashed lines perpendicular to the axis of the phase-sensitive measurement serve as a visual aid to emphasize the slant in the chirped case.

For comparison, the experiment was repeated without a chirped pump by removing the prism stretcher. A pulse shaper was used to select the bandwidth of the idler mode for the unchirped pump measurement to ensure matched JSI with the chirped pump case. The pulse shaper was fiber-coupled, adding additional dispersion to the light before the EOSI. This phase is well characterized and is compensated by the pulse shaper itself, as described in Refs. [23,24]. The joint spectral interference fringes depicted in Fig. 3 are not slanted as they are in the chirped pump case, pointing to the absence of phase correlations. We recovered a small but significant positive correlated phase $\phi_{11} = (7.4 \pm 1) \cdot 10^3\ \mathrm{fs}^2$ and $(5.5 \pm 2) \cdot 10^3\ \mathrm{fs}^2$ for the idler and signal passing through the EOSI, respectively. While small, these values are statistically significant and can be attributed to the pump pulses being slightly chirped at the point of the second harmonic generation process. The reconstructed local spectral phases were $\phi_{20} = (1.4 \pm 0.5) \cdot 10^4\ \mathrm{fs}^2$ for the idler and $\phi_{02} = (1.2 \pm 0.2) \cdot 10^4\ \mathrm{fs}^2$ for the signal, showing that the pulse shaper was close to compensating the large amount of dispersion caused by the optical fiber leading to the interferometer.

The complete JSA $f(\omega_1, \omega_2)$ for the cases of a chirped and a nearly transform-limited pump pulse was estimated from the joint EOSI data and is shown in Fig. 4. While the JSI distribution is nearly uncorrelated in both cases, the two-photon state for the case of a chirped pump exhibits significant spectral phase correlations encapsulated by the asymmetric saddle behavior. This distribution is not possible for a separable state and reveals entanglement from the spectral phase only. The magnitude of the JSAs differs between both cases because the prism compressor modifies the spatial mode of the pump and hence the interaction within the SPDC crystal, inducing weak amplitude correlations.

Since $f(\omega_1, \omega_2)$ is a function of two variables, it is possible to represent it in terms of a singular-value or Schmidt decomposition [29]. This represents $f(\omega_1, \omega_2)$ as a weighted sum of products of normalized Schmidt mode functions $\psi_i(\omega_1)$ and $\chi_i(\omega_2)$ (Supplement 1), where modes are numbered in decreasing

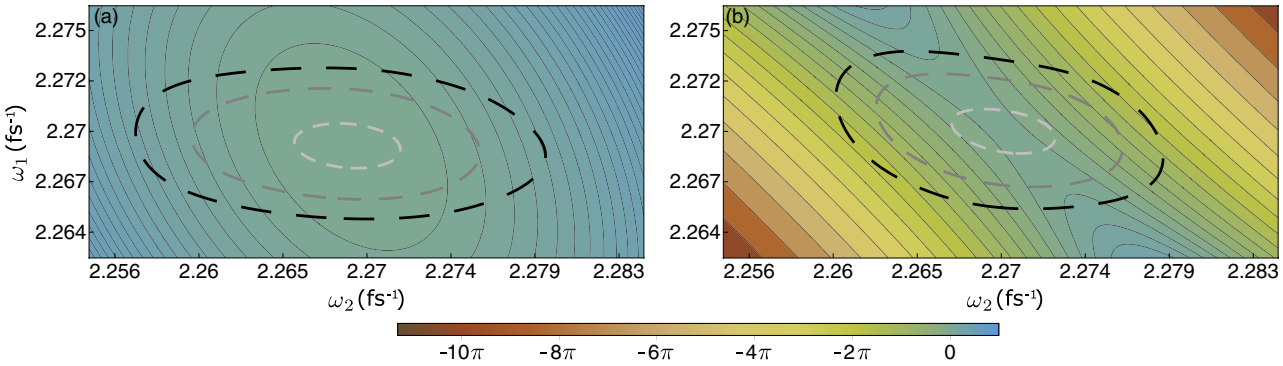

Fig. 4. Full phase-sensitive reconstruction of a two-photon joint spectral-temporal wave function, $f(\omega_1, \omega_2)$, for (a) an unchirped and (b) a chirped pump field. Background color indicates the phase of the complex JSA, $\mathrm{Arg}[f(\omega_1, \omega_2)]$ (plotted on an unwrapped scale), whilst the dotted contours show lines of constant amplitude $|f(\omega_1, \omega_2)|^2$. The state shown in (a) is nearly separable, whereas the nonlocal phase of the pump in (b) induces multimode entanglement.

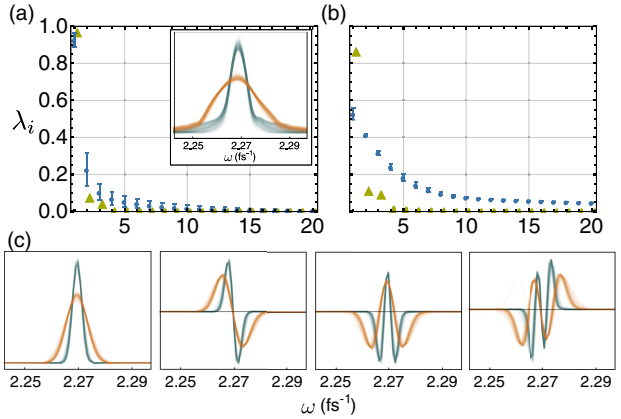

Fig. 5. Top: comparison of first 20 Schmidt coefficients of the measured complex JSA functions (a) with a nearly transform-limited pump and (b) with a chirped pump, illustrating the introduction of correlations. Green triangles represent Schmidt coefficients assuming flat phase distribution. Blue dots represent Schmidt coefficients calculated using the reconstructed phase distributions. Error bars are determined by the variance of Schmidt coefficients across the ensemble of reconstructions. (a) Inset: spectra of the dominant pair of normalized Schmidt modes with nearly transform-limited pump for signal (orange) and idler (cyan) photons. (c) Real part of the first four pairs of normalized Schmidt modes in the chirped-pump case (reconstructed from experimental data) for signal (orange) and idler (cyan) photons.

magnitude of the corresponding Schmidt coefficients. We use the effective Schmidt rank K as our measure of entanglement, with $K > 1$ indicating spectral-temporal entanglement (Supplement 1). The first 20 Schmidt coefficients are depicted in Fig. 4 for both the chirped and unchirped pump cases. As a comparison to illustrate the importance of spectral phase correlations, the Schmidt decomposition of the modulus of the JSA, $|f(\omega_1, \omega_2)|$, was also calculated in both cases.

The distribution of Schmidt coefficients when assuming a constant spectral phase is dominated by only a single term in both the transform-limited and chirped pump cases, with Schmidt number $K = 1.016$ and $K = 1.059$, respectively. When the measured joint spectral phase is taken into account, for the transform-limited pump case, the dominant Schmidt mode pair consists of the marginals of the JSA, $f(\omega_1, \omega_2) \approx \psi(\omega_1)\chi(\omega_2)$, with the Schmidt coefficients of the higher-order modes negligible, resulting in a Schmidt number $K = 1.2 \pm 0.2$. The measured nonlocal phase in the case of a chirped pump results in a highly multimode decomposition with the Schmidt number increased to $K = 5.0 \pm 0.5$. There are significant contributions from many Schmidt mode pairs for this state. The first four Schmidt modes are shown in Fig. 5, and their functional form resembles the first four Hermite–Gauss modes, as predicted when analyzing the output of SPDC [30]. These results confirm that when generating photon pairs using SPDC, controllable manipulation of the pump phase introduces spectral phase correlations in the daughter photons that influence the degree of two-photon entanglement. They furthermore highlight that to reveal this high-dimensional entanglement requires characterization of the joint spectral phase and not simply the JSI. We also note that given a well-known down-conversion process, the nonlocal phase of the daughter photon pair encodes the phase of the pump pulse and is invariant under local phase operations, suggesting a potential classical application in the characterization of ultraviolet pump pulses. Lastly, in directly measuring the full effect of pump chirp on the wave function of an SPDC photon pair for the first time, to the best of our knowledge, our work carries a result of direct interest to developers of PDC-based sources of quantum light.

4. CONCLUSION

To conclude, we have applied the technique of EOSI to demonstrate an original, highly flexible, and reference-free method to measure the global wave function of nonlocal quantum systems that exhibit entanglement across a high-dimensional basis. Since our method depends only on linear optical processes and has no need for an external optical reference, device implementations could be made quite compact and could characterize a larger ensemble of test states than other proposed approaches.

This demonstration, where control of the parameters of the source was shown to have a subtle but profound effect on the quantum properties of the output state, exemplifies the importance of a full characterization scheme in understanding the properties of quantum devices. In providing a tool for understanding and hence controlling the behavior of the elements of a quantum network, this approach has the potential to lead to transformative changes in high-dimensional quantum optical technologies such as TF-encoded crytography, simulation, metrology, and communications.

Funding. National Science Foundation (1620822); Horizon 2020 Framework Programme (665148); Defence Science and Technology Laboratory (DSTLX-100092545).

Acknowledgment. We are grateful to B. Brecht and M. Karpiński for fruitful discussions and insight on the results.

Disclosures. The authors declare no conflicts of interest.

See Supplement 1 for supporting content.

[†]These authors contributed equally to the paper.

REFERENCES

1. R. Horodecki, P. Horodecki, M. Horodecki, and K. Horodecki, "Quantum entanglement," Rev. Mod. Phys. **81**, 865–942 (2009).
2. R. Raussendorf, D. E. Browne, and H. J. Briegel, "Measurement-based quantum computation on cluster states," Phys. Rev. A **68**, 022312 (2003).
3. J. Nunn, L. J. Wright, C. Söller, L. Zhang, I. A. Walmsley, and B. J. Smith, "Large-alphabet time-frequency entangled quantum key distribution by means of time-to-frequency conversion," Opt. Express **21**, 15959–15973 (2013).
4. C. H. Bennett, P. W. Shor, J. A. Smolin, and A. V. Thapliyal, "Entanglement-assisted classical capacity of noisy quantum channels," Phys. Rev. Lett. **83**, 3081–3084 (1999).
5. C. Wang, F.-G. Deng, Y.-S. Li, X.-S. Liu, and G. L. Long, "Quantum secure direct communication with high-dimension quantum superdense coding," Phys. Rev. A **71**, 044305 (2005).
6. M. Horodecki, "Entanglement measures," Quantum Inf. Comput. **1**, 3–26 (2001).
7. P. G. Kwiat, K. Mattle, H. Weinfurter, A. Zeilinger, A. V. Sergienko, and Y. Shih, "New high-intensity source of polarization-entangled photon pairs," Phys. Rev. Lett. **75**, 4337–4341 (1995).
8. G. Molina-Terriza, J. P. Torres, and L. Torner, "Twisted photons," Nat. Phys. **3**, 305–310 (2007).

9. B. Brecht, D. V. Reddy, C. Silberhorn, and M. G. Raymer, "Photon temporal modes: a complete framework for quantum information science," Phys. Rev. X **5**, 041017 (2015).
10. W. Tittel, J. Brendel, H. Zbinden, and N. Gisin, "Quantum cryptography using entangled photons in energy-time bell states," Phys. Rev. Lett. **84**, 4737–4740 (2000).
11. V. Giovannetti, S. Lloyd, and L. Maccone, "Advances in quantum metrology," Nat. Photonics **5**, 222–229 (2011).
12. M. G. Raymer, A. H. Marcus, J. R. Widom, and D. L. P. Vitullo, "Entangled photon-pair two-dimensional fluorescence spectroscopy (EPP-2DFS)," J. Phys. Chem. B **117**, 15559–15575 (2013).
13. M. Lanzagorta, "Low-brightness quantum radar," Proc. SPIE **9461**, 946113 (2015).
14. A. C. Dada, J. Leach, G. S. Buller, M. J. Padgett, and E. Andersson, "Experimental high-dimensional two-photon entanglement and violations of generalized bell inequalities," Nat. Phys. **7**, 677–680 (2011).
15. K. Zielnicki, K. Garay-Palmett, D. Cruz-Delgado, H. Cruz-Ramirez, M. F. O'Boyle, B. Fang, V. O. Lorenz, A. B. U'Ren, and P. G. Kwiat, "Joint spectral characterization of photon-pair sources," J. Mod. Opt. **65**, 1141–1160 (2018).
16. J. Lundeen, A. Feito, H. Coldenstrodt-Ronge, K. Pregnell, C. Silberhorn, T. Ralph, J. Eisert, M. Plenio, and I. Walmsley, "Tomography of quantum detectors," Nat. Phys. **5**, 27–30 (2009).
17. N. Killoran and N. Lütkenhaus, "Strong quantitative benchmarking of quantum optical devices," Phys. Rev. A **83**, 052320 (2011).
18. O. Kuzucu, F. N. Wong, S. Kurimura, and S. Tovstonog, "Joint temporal density measurements for two-photon state characterization," Phys. Rev. Lett. **101**, 153602 (2008).
19. J.-P. W. MacLean, J. M. Donohue, and K. J. Resch, "Direct characterization of ultrafast energy-time entangled photon pairs," Phys. Rev. Lett. **120**, 053601 (2018).
20. P. Chen, C. Shu, X. Guo, M. M. T. Loy, and S. Du, "Measuring the biphoton temporal wave function with polarization-dependent and time-resolved two-photon interference," Phys. Rev. Lett. **114**, 010401 (2015).
21. N. Tischler, A. Buese, L. G. Helt, M. L. Juan, N. Piro, J. Ghosh, M. J. Steel, and G. Molina-Terriza, "Measurement and shaping of biphoton spectral wave functions," Phys. Rev. Lett. **115**, 193602 (2015).
22. J.-P. W. MacLean, S. Schwarz, and K. J. Resch, "Reconstructing ultrafast energy-time entangled two-photon pulses," Phys. Rev. A **100**, 033834 (2019).
23. A. Davis, V. Thiel, M. Karpiński, and B. Smith, "Measuring the single photon spectral-temporal wave function," Phys. Rev. Lett. **121**, 083602 (2018).
24. A. Davis, V. Thiel, M. Karpiński, and B. Smith, "Experimental single-photon pulse characterization by electro-optic shearing interferometry," Phys. Rev. A **98**, 023840 (2018).
25. C. Dorrer and I. Kang, "Highly sensitive direct characterization of femtosecond pulses by electro-optic spectral shearing interferometry," Opt. Lett. **28**, 477–479 (2003).
26. I. Walmsley and C. Dorrer, "Characterization of ultrashort electromagnetic pulses," Adv. Opt. Photon. **1**, 308–437 (2009).
27. P. J. Mosley, J. S. Lundeen, B. J. Smith, P. Wasylczyk, A. B. U'Ren, C. Silberhorn, and I. A. Walmsley, "Heralded generation of ultrafast single photons in pure quantum states," Phys. Rev. Lett. **100**, 133601 (2008).
28. A. Davis, P. Saulnier, M. Karpiński, and B. Smith, "Pulsed single-photon spectrometer by frequency-to-time mapping using chirped fiber Bragg gratings," Opt. Express **25**, 12804–12811 (2017).
29. A. Peres, *Quantum Theory: Concepts and Methods* (Springer, 2006), Vol. **57**.
30. F. Arzani, C. Fabre, and N. Treps, "Versatile engineering of multimode squeezed states by optimizing the pump spectral profile in spontaneous parametric down-conversion," Phys. Rev. A **97**, 033808 (2018).